

# A Local Signal based Inter-area Damping Controller via Dynamic State Estimation Approach

Qi Zeng, Ziyu Fan, Lin Jiang, *Member, IEEE*

**Abstract**—To suppress inter-area oscillations and enhance small-signal stability of power systems, wide-area damping controllers (WADC) have been used by utilising wide-area signals with high observabilities to inter-area modes. However, the requirement of the wide-area signal makes communication systems involved in the control loops of the power systems and therefore, the damping performance of the conventional WADC suffers from time-delay, data dropout and cyber-attacks. This paper proposes a local signal based inter-area damping controller (LSIADC) to suppress inter-area oscillation without using wide-area signals. The LSIADC extracts a signal with high observability to the inter-area mode from the local signal by dynamic state estimation (DSE) technique and the control signal is obtained by adding a proper phase shift to the extracted signal. The simulation results show that the proposed controller can effectively suppress inter-area oscillation using the local signal only.

**Index Terms**—Power system stability, inter-area oscillation damping, dynamic states estimation, extended Kalman filter

## I. INTRODUCTION

Inter-area oscillation is one of the major stability concerns of nowadays large-scale power systems because of the long transmission distance between the generation site and the load centre, as well as the tension of operating the power system closed to its operating margin for a maximum revenue under a competing market environment [1]. Inter-area oscillations can be damped by power system stabilisers (PSS) for synchronous generators and supplementary damping controllers (SDC) for flexible alternating current transmission (FACT) devices [2]. Due to the lack of observability from the local measurements to the inter-area modes, those local signal based controllers may not provide sufficient damping to the inter-area oscillation modes. With the development of wide-area measurement systems (WAMS) based on synchronised phasor measurement units (PMU) and communication network, the remote signals with direct representation of the oscillation modes have been applied to design wide-area damping controllers (WADC) to damp inter-area oscillations [1], [3], [4], [5], [6].

Despite WADC providing better performance on suppressing inter-area oscillation, the remote signal based controllers involve the communication system in the control loop and introduce several impacts degrading the dynamic performance, including time delay, data packets' mis-order, drop-out, and the worst-case such as loss of remote signal caused by physical failure of communication networks and faked remote signal

from malicious cyber-attacks. Lots of research have been done in the stability analysis and controller synthesis of the WADC considering the impact of time delay and the data packet drop-out of the remote signal [7], [8]. Recently, increased efforts have been proposed to detect and mitigate the negative impact of signal loss and faked signal in the design stage of the WADC, mainly using the following three categories of methods, i.e., robust method [8], redundant remote signals based methods[9], and signal reconstruction based methods [10].

In [8], a controller based on robust method using both the local and remote signal as the feedback inputs under the healthy communication networks is proposed to deal with the loss of remote signal as parts of uncertainties. Redundant remote signals are used by the controller in [9] to replace the lost or faulty remote signal after the communication fault or cyber-attack is detected. Besides, the fault or faked signals can be replaced via signal reconstruction by model-based state estimation method [10], in which the dynamic state estimation (DSE) technique is used to reconstruct the signal and a DSE-based WADC to enhance the damping performance of power systems considering communication fault. This approach uses a forecasting-aided state estimation (FASE) to obtain the control signal of the SDC on a static var compensator (SVC), then, the FASE-WADC can enhance the damping performance.

DSE has been used for enhancing the performance of control systems of power systems and improving the reliability of power systems and the dynamic states obtained from DSE enables the design of effective wide-area controllers [11], [12], [13]. Besides, DSE based control approaches have been proposed for better control and online monitoring of power system by using estimation of wide-area dynamic states [14], wide-area signal [10] and recovering missing data [15]. In this paper, a local signal based inter-area damping controller (LSIADC) is proposed to suppress inter-area oscillation using local signal via DSE technique. In [16], the DSE has been used for the detection of inter-area oscillations using an extended Kalman filter (EKF). However, [16] focus on the monitoring the frequency and damping of the oscillation while other estimation results are ignored. This paper uses all estimation results in a continuous EKF to represent an oscillation signal. This oscillation signal is extracted from a local signal and has high observability to the inter-area mode. By a further transformation, the extracted signal can be expressed as the projection of an estimated phasor which is proved to be same as the phasor in [17], [18]. Thus, the control signal can be obtained by adding a proper phase shift to the extracted

Q. Zeng, Z. Fan, L. Jiang are with the Department of Electrical Engineering and Electronics, University of Liverpool, Liverpool, L69 3GJ, United Kingdom (email: psqzeng2@liverpool.ac.uk; Ziyu.Fan@liverpool.ac.uk; ljiang@liv.ac.uk).

signal. Different from the existing method [18], this paper uses the model-based residue method to calculate the proper phase shift. Compared to the existing DSE based approaches, the proposed LSIADC release the requirement of wide-area signal to suppress inter-area oscillation while LSIADC has a similar control performance and control effort. Therefore, the LSIADC will not suffer from time-delay, packet loss and cyber-attack.

The main contributions of this paper can be summarised as:

- This paper proposes a damping controller using the local signal only. The proposed controller can suppress the inter-area oscillation effectively without interference from time delay, packet loss and cyber-attack.
- This controller separates the inter-area modes from the local signal using a continuous EKF. The extracted oscillation signal can be used to suppress inter-area oscillation after compensating a phase shift.
- Based on the direct representation of inter-area mode using local signal, the optimal phase shift for the proposed LSIADC can be determined by the model-based residue method.

The rest of this paper is organised as followed: In Section II, the scheme and the algorithm of the proposed controller are presented. The case studies based on New England 10-machine 39-bus power system will be carried out in Section III. The conclusions are given in Section IV.

## II. THE SCHEME OF THE LOCAL SIGNAL BASED INTER-AREA DAMPING CONTROLLER

In this section, the overall scheme of the LSIADC will be illustrated. The scheme of the conventional WADC (C-WADC) is shown in Fig.1(a), which utilise a remote signal as the feedback. Different from the C-WADC, the proposed controller utilises the active power of the local generator as input and the control signal is fed into the AVR of local generator as shown in Fig.1(b).

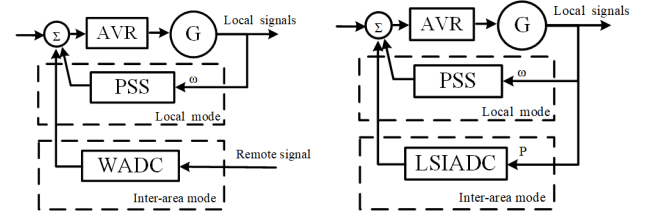
The structures of the C-WADC and the proposed LSIADC are given in Fig.1(c) and Fig.1(d), respectively, and the block diagram of the proposed LSIADC is given in the 2. The C-WADC is composed of a gain block, a washout filter and lead-lag blocks to compensate the phase of feedback signal [7]. The proposed LSIADC is composed of a gain block, a Kalman filter and lead-lag blocks. The Kalman filter is used to extract the oscillation signal from the local signal (the active power of the local generator), as shown in the left part of the 2. The control signal can be obtained by compensating a proper phase shift to the extracted oscillation signal by the lead-lag blocks, as shown in the right part of the 2.

### A. Expressing the oscillation by exponentially damped signals

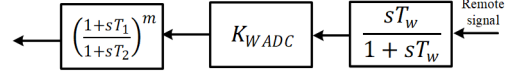
This section will introduce how to present the oscillatory signal as an exponentially damped sinusoidal signal. For a linear system,

$$\dot{x} = Ax + Bu \quad (1)$$

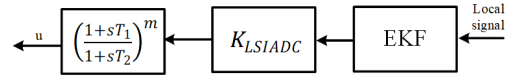
$$y = Cx \quad (2)$$



(a) The generator equipped with a C-WADC. (b) The generator equipped with a LSIADC.



(c) The structure of the C-WADC.



(d) The structure of the LSIADC.

Fig. 1. Comparison of the C-WADC and LSIADC.

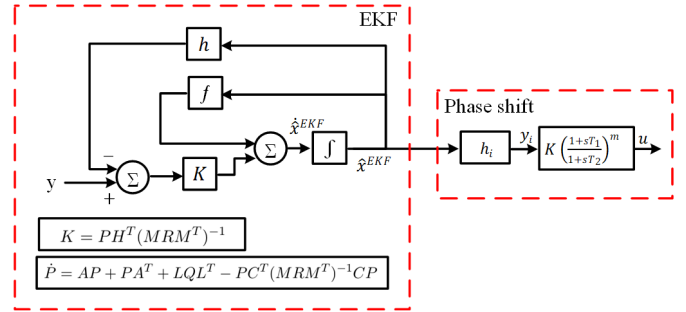


Fig. 2. The block diagram of the proposed LSIADC.

where  $x, y, u$  are the system state, the measurement and the input, respectively.  $A, B, C$  are the system matrix, input matrix and the measurement matrix, respectively. According to modal analysis theory, the measurement can be expressed as the sum of  $N$  oscillation modes of the system [2].

$$y(t) = C \sum_{i=1}^N V_i z_i(0) e^{\lambda_i t} \quad (3)$$

where  $V_i$  is the  $i^{th}$  row of the left eigenvector of the matrix  $A$ ,  $z_i(0)$  is the initial value of  $i^{th}$  oscillation mode,  $\lambda_i$  is the eigenvalue of the  $i^{th}$  mode. In Eq.(3), letting

$$\lambda_i = \sigma_i + j\omega_i \quad (4)$$

$$CV_i z_i(0) = a_i + jb_i \quad (5)$$

where  $\sigma_i, \omega_i$  are the damping and the frequency of the  $i^{th}$  mode, respectively. The oscillation modes appear as complex conjugate pairs and denote that the  $i^{th}$  mode and the  $(i+1)^{th}$  mode are conjugated. Then the contribution from  $i^{th}$  and  $(i+1)^{th}$  modes to the measured oscillation signal is

$$y_i(t) = (a_i - jb_i) e^{(\sigma_i - j\omega_i)t} + (a_i + jb_i) e^{(\sigma_i + j\omega_i)t} \quad (6)$$

$$= 2ae^{\sigma_i t} \cos(\omega_i t) - 2be^{\sigma_i t} \sin(\omega_i t) \quad (6)$$

$$= A_i e^{\sigma_i t} [\cos \phi_i \cos(\omega_i t) - \sin \phi_i \sin(\omega_i t)] \quad (7)$$

$$= A_i e^{\sigma_i t} \cos(\omega_i t + \phi_i) \quad (8)$$

Where  $A_i = 2\sqrt{a_i^2 + b_i^2}$  and  $\tan(\phi_i) = b_i/a_i$ . The coefficients of this exponentially damped signal (EDS), i.e.  $a$  and  $b$

depend on the system model ( $C, V$  and  $\lambda$ ) and the initial state of the oscillation mode  $z(0)$ . Based on Eq.(7), the space-space model of the signal will be built and the transformation to the phasor representing the inter-area oscillation is based on Eq.(6).

### B. Extracting the oscillation signal from the local signal

Secondly, the DSE approach for extracting the oscillation signal associated to inter-area modes using continuous EKF is introduced. The Kalman filter is an optimal estimator to estimate the system state that minimises the mean square of the estimation error in the presence of white noise using the nonlinear signal model and the signal measurements. Define  $4N$  state variables of the signal as

$$x_{4i-3}^{EKF} = A_i e^{\sigma_i t} \cos(\omega_i t) \quad (9)$$

$$x_{4i-2}^{EKF} = A_i e^{\sigma_i t} \sin(\omega_i t) \quad (10)$$

$$x_{4i-1}^{EKF} = \omega_i \quad (11)$$

$$x_{4i-0}^{EKF} = \sigma_i \quad (12)$$

The system function can be expressed as

$$\begin{aligned} \dot{\hat{x}}_{4i-3}^{EKF} &= A_i \sigma_i e^{\sigma_i t} \cos(\omega_i t) - A_i \omega_i e^{\sigma_i t} \sin(\omega_i t) + w_1 \\ &= x_{4i-0}^{EKF} x_{4i-3}^{EKF} - x_{4i-1}^{EKF} x_{4i-2}^{EKF} + w_1 \end{aligned} \quad (13)$$

$$\begin{aligned} \dot{\hat{x}}_{4i-2}^{EKF} &= A_i \sigma_i e^{\sigma_i t} \sin(\omega_i t) + A_i \omega_i e^{\sigma_i t} \cos(\omega_i t) + w_2 \\ &= x_{4i-2}^{EKF} x_{4i-0}^{EKF} - x_{4i-3}^{EKF} x_{4i-1}^{EKF} + w_2 \end{aligned} \quad (14)$$

$$\dot{\hat{x}}_{4i-1}^{EKF} = w_3 \quad (15)$$

$$\dot{\hat{x}}_{4i-0}^{EKF} = w_4 \quad (16)$$

According to Eq.(7), the measurement function can be expressed as:

$$y = \sum_{i=1}^n \{ \cos(\phi_i) x_{4i-3}^{EKF} - \sin(\phi_i) x_{4i-2}^{EKF} + v \} \quad (17)$$

The  $\hat{x}_{4i-3}^{EKF}$  and  $\hat{x}_{4i-2}^{EKF}$  are in-phase and quadrature components of the signal, respectively; The  $\hat{x}_{4i-1}^{EKF}$  and  $\hat{x}_{4i-0}^{EKF}$  are the frequency and damping factor of the  $i^{th}$  oscillation mode, respectively;  $w$  and  $v$  are process noise and measurement noise, respectively. The noises are uncorrelated zero-mean white noises and satisfy  $E[ww^T] = Q$  and  $E[vv^T] = R$ . Note that the update of  $\hat{x}_{4i-1}^{EKF}$  and  $\hat{x}_{4i-0}^{EKF}$  are based on the noise matrix  $Q$ . Consider the nonlinear system described in Eq.(9)-(17),

$$\dot{\hat{x}}^{EKF} = f(\hat{x}^{EKF}) + w \quad (18)$$

$$y = h(\hat{x}^{EKF}) + v \quad (19)$$

where  $f(\cdot)$  and  $h(\cdot)$  are the nonlinear system function and measurement function, respectively. Then, the continuous EKF can be expressed as

$$\dot{\hat{x}}^{EKF} = f(\hat{x}^{EKF}, u, t) + K [y - h(\hat{x}^{EKF}, t)] \quad (20)$$

$$K = PH^T(R)^{-1} \quad (21)$$

$$\dot{P} = FP + PF^T + Q - PH^T(R)^{-1}HP \quad (22)$$

where  $K$  is the Kalman gain matrix at time  $k$ ,  $F$  and  $H$  are the Jacobin matrices of system function  $f$  and measurement function  $h$ , respectively, which can be computed by  $F_{k-1} = \left. \frac{\partial f}{\partial x} \right|_{x=\hat{x}(t)}$ ,  $H_k = \left. \frac{\partial h}{\partial x} \right|_{x=\hat{x}(t)}$ . Then, considering  $n$  modes of the system, the system function and measurement function are

$$f(x) = \begin{bmatrix} M_1 \\ \vdots \\ M_i \\ \vdots \\ M_N \end{bmatrix}, \text{ where } M_i = \begin{bmatrix} \dot{\hat{x}}_{4i-3}^{EKF} \\ \dot{\hat{x}}_{4i-2}^{EKF} \\ \dot{\hat{x}}_{4i-1}^{EKF} \\ \dot{\hat{x}}_{4i-0}^{EKF} \end{bmatrix} \quad (23)$$

$$h(\hat{x}^{EKF}) = H \hat{x}^{EKF} \quad (24)$$

$$H = [k_1 \ k_2 \ 0 \ 0 \ \dots \ k_{2N-1} \ k_{2N} \ 0 \ 0] \quad (25)$$

where  $k_{2i-1} = \cos(\phi_i)$  and  $k_{2i} = -\sin(\phi_i)$ . Then, the extracted oscillation signal is the  $i^{th}$  term of Eq.(17) and it can be express as:

$$y_i = h_i(\hat{x}^{EKF}) = \cos(\phi_i) x_{4i-3}^{EKF} - \sin(\phi_i) x_{4i-2}^{EKF} \quad (26)$$

As shown by Eq.(13) - Eq.(16) and Eq.(25), the EKF is designed to estimate the parameters of  $n$  dominated modes from the local signal separately and the Eq.(26) is the critical mode among  $n$  modes.

### C. Suppressing the inter-area oscillation using the extracted signal

Thirdly, how to suppress the inter-area oscillation using the extracted oscillation signal will be demonstrated. The two terms in Eq.(26) can be treated as d/q components of a phasor, then  $y_i$  is the real part of this phasor. Using the extracted phasor to suppress inter-area oscillation has been introduced and commercialised by ABB [17]. The oscillation signal being expressed as a sum of EDS can be re-written in a phasor form [18]:

$$y(t) = y_{av}(t) + \text{Real} \sum_{i=1}^n \{ \vec{y}_i e^{j\omega_i t} \} \quad (27)$$

where  $y_{av}$  is the average part of the signal  $y(t)$ ,  $\vec{y}_i$  is a phasor that represents the  $i^{th}$  oscillation in a coordinate system rotating with angular frequency  $\omega_i$ . The real part of the  $i^{th}$  phasor can be expressed as the following equation based on the transformation based on Eq.(6)-Eq.(8).

$$\text{Real}\{ \vec{y}_i e^{j\omega_i t} \} = y_d(t) \cos \omega t - y_q(t) \sin \omega t \quad (28)$$

$$= 2a_i e^{\sigma_i t} \cos(\omega_i t) - 2b_i e^{\sigma_i t} \sin(\omega_i t) \quad (29)$$

$$= \cos(\phi_i) \hat{x}_{4i-3}^{EKF} - \sin(\phi_i) \hat{x}_{4i-2}^{EKF} \quad (30)$$

Then according to [17], [18], the control signal can be obtained by applying a proper phase shift and gain to the phasor  $\vec{y}_i$ .

$$\begin{bmatrix} u(t) \\ \backslash \end{bmatrix} = K \begin{bmatrix} \cos \beta & -\sin \beta \\ \sin \beta & \cos \beta \end{bmatrix} \begin{bmatrix} \cos \phi_i & -\sin \phi_i \\ \sin \phi_i & \cos \phi_i \end{bmatrix} \begin{bmatrix} \hat{x}_{4i-3}^{EKF} \\ \hat{x}_{4i-2}^{EKF} \end{bmatrix} \quad (31)$$

where  $\beta$  is the phase shift for suppressing the inter-area oscillation.

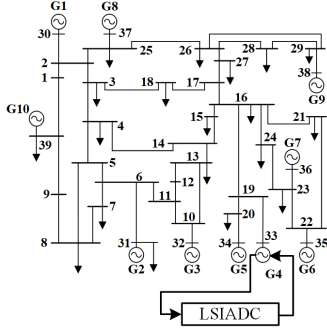


Fig. 3. The New England 10-machine 39-bus power system equipped with the proposed LSIADC.

TABLE I  
THE INTER-AREA OSCILLATION MODES ACCORDING TO THE SMALL-SIGNAL STABILITY ANALYSIS.

	$f$	$\sigma$	Dominant Generator
Mode 1	1.054	0.03	G1 vs all
Mode 2	1.005	0.04	(4,5,6,7) vs (2,3) vs (8,9,10)
Mode 3	0.657	0.04	(2,3) vs (8,9,10)

#### D. Determining the phase shift

The phase shift  $\beta$  can be determined using the model-based residue method [1]. The  $k^{th}$  output is selected as the extracted oscillation signal  $y_i(t) = \cos(\phi_i)\hat{x}_{4i-3}^{EKF} - \sin(\phi_i)\hat{x}_{4i-2}^{EKF}$ . The  $j^{th}$  input is selected as the voltage fed into the excitation system of the local generator. The  $i^{th}$  mode is the critical inter-area oscillation mode. If the residue  $R_{ijk}$  obtained from the linearization analysis is associated to the  $k^{th}$  output,  $j^{th}$  input and  $i^{th}$  mode, and the transfer function of the lead-lag blocks is  $KH_i(s)$ , then the lead-lag blocks for phase shift can be designed as:

$$KH(s) = K \frac{sT_w}{1 + sT_w} \left[ \frac{1 + sT_1}{1 + sT_2} \right]^m \quad (32)$$

where  $T_w$  is the parameter for a washout filter;  $T_1$  and  $T_2$  are the parameters for the phase shift. The phase compensation method is an existing approach and the calculation of the parameters is omitted due to page limit. The calculation method can be found in [1].

### III. CASE STUDIES

Simulations on 10-machine 39-bus power system as shown in Fig.3 are carried out to verify the effectiveness of the proposed LSIADC. In this power system, the LSIADC is installed at the G4 and the control signal is fed into the AVR of G4. The extracted signal is extracted from the local signal, i.e. the active power of the G4:  $P_4$ . As the comparison, the remote signal for the conventional WADC, robust WADC and DSE based WADC is selected as the active power between bus 3 and bus 18:  $P_{3-18}$ .

#### A. Designing the LSIADC

Firstly, the model of the power system is linearised at an operation point. The small signal stability analysis is carried out and the results are given in Table I. The inter-area mode 3 at 0.657Hz is the critical inter-area oscillation mode to be suppressed. Then, the results of the small signal stability analysis are used to implement the EKF as described in Section

TABLE II  
THE RESULTS OF THE OBSERVABILITY ANALYSIS TO THE INTER-AREA OSCILLATION MODES.

	Mode 1	Mode 2	Mode 3
Local signal ( $P_4$ )	0.0667	0.1327	0.1386
Remote signal ( $P_{3-18}$ )	0.2119	0.3225	0.8732
Extracted signal	0.1664	0.3651	1

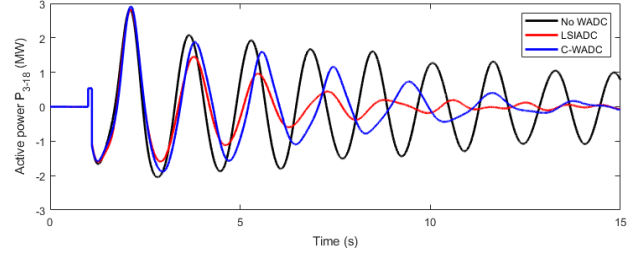


Fig. 4. The system response of active power deviation  $P_{3-18}$  when the system is equipped with LSIADC compared to C-WADC.

II. Thirdly, the residue method is used to calculate the phase shift of the extracted signal. Note that the proposed method cannot identify a mode if the observability of the local signal to this mode is zero and we assume that the local signal from this generator has little but enough observability for the extraction of the critical inter-area oscillation.

#### B. Simulation results

After the implementation of the controller, the observability analysis is also carried out and the result is given in Table II. As shown in the table, the local signal has low observability to the inter-area mode 3. The remote signal  $P_{3-18}$  has higher observability to this mode and makes it a better candidate of feedback signal. Furthermore, the extracted signal has highest observability than the remote signal which means that it is a better choice compared to  $P_{3-18}$ .

The simulation results are given in Fig.4 - Fig.6. The disturbance is set as: a three-phase grounding fault between bus #2 and #3 is added at  $t = 1.0s$  and cleared at  $t = 1.1s$ . The active power  $P_{3-18}$  will be used to illustrate the effectiveness of the controller.

Fig.4 shows the active power deviation  $P_{3-18}$  when the system is equipped with LSIADC compared to a C-WADC. Compared to the C-WADC, the proposed LSIADC can provide better damping performance. Fig.5 shows the comparison to the robust WADC (R-WADC) and DSE based WADC (DSE-WADC) designed in [8] and [10], respectively. The R-WADC uses both the local and the remote signals as the input. When both signals are available, the R-WADC can provide good

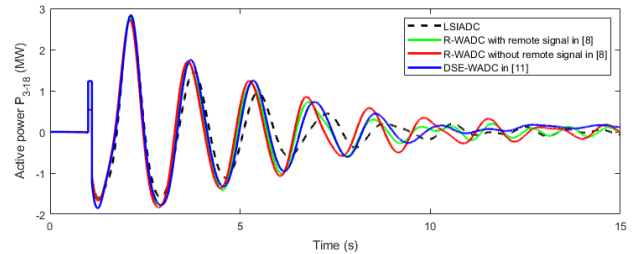
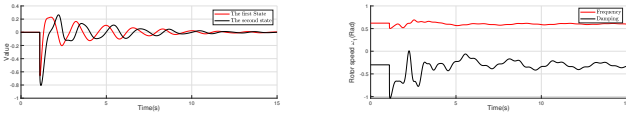
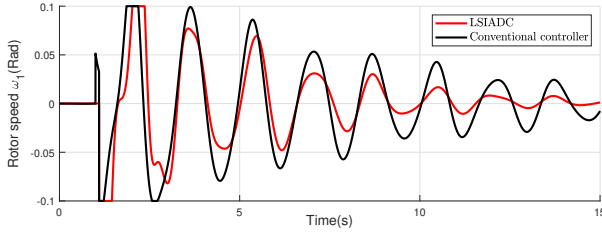


Fig. 5. The system response of active power deviation  $P_{3-18}$  when the system is equipped with LSIADC compared to R-WADC and DSE-WADC.



(a) The first and the second states of the critical inter-area oscillation. (b) The frequency and the damping of the critical inter-area oscillation.



(c) The output of the proposed LSIADC and the C-WADC.

Fig. 6. The performance of the DSE in the proposed LSIADC.

damping performance while when the remote signal is lost, the R-WADC can still provide satisfied damping performance. The R-WADC can suppress inter-area oscillation using local signal only, however, R-WADC consider the robustness to the worst condition. This makes it degraded damping performance even under normal condition. As shown in the Fig.5, the proposed LSIADC can provide better damping performance compared to R-WADC even when R-WADC uses both of the local and the remote signals as shown by the red line. Compared to the DSE-WADC, the proposed LSIADC has similar damping performance without the requirement of the wide-area signal while the DSE-WADC in [10] requires 304 PMUs in 50-generator power system.

The Fig.6(a)-Fig.6(c) provide the performance of the DSE. As we can see, the proposed LSIADC can provide damping performance as good as that of recent research with similar control effort. Fig.6(a) shows the first and the second estimated states of the inter-area oscillation, i.e.,  $x_{4i-3}^{EKF}$  and  $x_{4i-2}^{EKF}$  in Eq.(31). Fig.6(b) provides the tracked frequency and the damping of the inter-area oscillation and Fig.6(b) provides the output of the proposed LSIADC and the C-WADC. Note that even without the actual frequency and damping factor, the estimated parameter will still converge to their actual values because the EKF will update the estimation results according to difference between the measured signal  $y(t)$  and estimated signal  $h(\hat{x}^{EKF}, t)$ . However, the simulation to verify is omitted due to page limitation.

#### IV. CONCLUSION

This paper proposes a novel local signal based inter-area damping controller. The proposed controller extracts the inter-area modes from local signal. The extracted signal has high observability to the critical inter-area mode such that the proposed controller is able to suppress inter-area oscillation using local signal only by adding a proper phase shift to the extracted signal. Without the communication system in the control loop, the damping performance is immune to time delay, communication fault and cyber attack. Simulation results shows that the proposed LSIADC can provide better

damping performance compared to C-WADC, R-WADC and DSE-WADC although the proposed controller uses local signal only.

#### REFERENCES

- [1] M. E. Aboul-Ela, A. A. Sallam, J. D. McCalley, and A. A. Fouad, "Damping controller design for power system oscillations using global signals," *IEEE Transactions on Power Systems*, vol. 11, no. 2, pp. 767–773, may 1996.
- [2] P. Kundur, *Power System Stability and Control*. McGraw-Hill, 1994.
- [3] N. Yang, Q. Liu, and J. D. McCalley, "TCSC controller design for damping interarea oscillations," *IEEE Transactions on Power Systems*, vol. 13, no. 4, pp. 1304–1310, 1998.
- [4] Y. Zhang and A. Bose, "Design of wide-area damping controllers for interarea oscillations," *IEEE Transactions on Power Systems*, vol. 23, no. 3, pp. 1136–1143, aug 2008.
- [5] W. Yao, L. Jiang, J. Wen, Q. H. Wu, and S. Cheng, "Wide-area damping controller of Facts devices for inter-area oscillations considering communication time delays," *IEEE Transactions on Power Systems*, vol. 29, no. 1, pp. 318–329, jan 2014.
- [6] X. Zhang, C. Lu, S. Liu, and X. Wang, "A review on wide-area damping control to restrain inter-area low frequency oscillation for large-scale power systems with increasing renewable generation," *Renewable and Sustainable Energy Reviews*, vol. 57, pp. 45–58, 2016.
- [7] W. Yao, L. Jiang, Q. H. Wu, J. Y. Wen, and S. J. Cheng, "Delay-dependent stability analysis of the power system with a wide-area damping controller embedded," *IEEE Transactions on Power Systems*, vol. 26, no. 1, pp. 233–240, 2011.
- [8] S. Zhang and V. Vittal, "Design of wide-area power system damping controllers resilient to communication failures," *IEEE Transactions on Power Systems*, vol. 28, no. 4, pp. 4292–4300, nov 2013.
- [9] S. Zhang and V. Vittal, "Wide-area control resiliency using redundant communication paths," *IEEE Transactions on Power Systems*, vol. 29, no. 5, pp. 2189–2199, sep 2014.
- [10] I. L. Ortega Rivera, V. Vittal, G. T. Heydt, C. R. Fuerte-Esquivel, and C. Angeles-Camacho, "A dynamic state estimator based control for power system damping," *IEEE Transactions on Power Systems*, vol. 33, no. 6, pp. 6839–6848, nov 2018.
- [11] J. Zhao, A. Gómez-Expósito, M. Netto, L. Mili, A. Abur, V. Terzija, I. Kamwa, B. Pal, A. K. Singh, J. Qi, Z. Huang, and A. P. Meliopoulos, "Power System Dynamic State Estimation: Motivations, Definitions, Methodologies, and Future Work," *IEEE Transactions on Power Systems*, vol. 34, no. 4, pp. 3188–3198, jul 2019.
- [12] Y. Liu, A. K. Singh, J. Zhao, A. P. S. Meliopoulos, B. Pal, M. A. b. M. Ariff, T. Van Cutsem, M. Glavic, Z. Huang, I. Kamwa, L. Mili, A. S. Mir, A. Taha, V. Terzija, and S. Yu, "Dynamic State Estimation for Power System Control and Protection IEEE Task Force on Power System Dynamic State and Parameter Estimation," *IEEE Transactions on Power Systems*, vol. 36, no. 6, pp. 5909–5921, nov 2021.
- [13] J. Zhao, M. Netto, Z. Huang, S. S. Yu, A. Gomez-Exposito, S. Wang, I. Kamwa, S. Akhlaghi, L. Mili, V. Terzija, A. P. S. Meliopoulos, B. Pal, A. K. Singh, A. Abur, T. Bi, and A. Rouhani, "Roles of Dynamic State Estimation in Power System Modeling, Monitoring and Operation," *IEEE Transactions on Power Systems*, vol. 36, no. 3, pp. 2462–2472, may 2021.
- [14] A. K. Singh and B. C. Pal, "Decentralized Nonlinear Control for Power Systems Using Normal Forms and Detailed Models," *IEEE Transactions on Power Systems*, vol. 33, no. 2, pp. 1160–1172, 2018.
- [15] J. Zhao and L. Mili, "Power System Robust Decentralized Dynamic State Estimation Based on Multiple Hypothesis Testing," *IEEE Transactions on Power Systems*, vol. 33, no. 4, pp. 4553–4562, 2018.
- [16] M. Yazdani, A. Mehrizi-Sani, and M. Mojiri, "Estimation of Electromechanical Oscillation Parameters Using an Extended Kalman Filter," *IEEE Transactions on Power Systems*, vol. 30, no. 6, pp. 2994–3002, 2015.
- [17] L. Ångquist and C. Gama, "Damping algorithm based on phasor estimation," *Proceedings of the IEEE Power Engineering Society Transmission and Distribution Conference*, vol. 3, no. WINTER MEETING, pp. 1160–1165, 2001.
- [18] N. R. Chaudhuri, S. Ray, R. Majumder, and B. Chaudhuri, "A New Approach to Continuous Latency Compensation With Adaptive Phasor Power Oscillation Damping Controller (POD)," *IEEE Transactions on Power Systems*, vol. 25, no. 2, pp. 939–946, may 2010.